Generalized gradient approximations with local parameters

Angel Albavera-Mata,[1] Karla Botello-Mancilla,[2] S. B. Trickey,[3] José L. Gázquez,[4] and Alberto Vela[1,*]

[1]*Departamento de Química, Centro de Investigación y de Estudios Avanzados, Avenida Instituto Politécnico Nacional 2508, 07360 Ciudad de México, México*

[2]*Escuela Superior de Ingeniería Química e Industrias Extractivas, Instituto Politécnico Nacional, Avenida Luis Enrique Erro SN, 07738 Ciudad de México, México*

[3]*Quantum Theory Project, Department of Physics and Department of Chemistry, University of Florida, P.O. Box 118435, Gainesville, Florida 32611-8435, USA*

[4]*Departamento de Química, Universidad Autónoma Metropolitana Iztapalapa, Avenida San Rafael Atlixco 186, 09340 Ciudad de México, México*

(Received 6 February 2020; accepted 30 June 2020; published 16 July 2020)

We develop and demonstrate the performance of a nonseparable form of the generalized gradient approximation (GGA) for exchange and correlation that includes locally varying parameters that match second-order gradient expansion behavior. Specifically, the high- and low-density limits are included to recover locally the linear response through inclusion of their dependence on the electron density. This local parametrization allows the GGA form to provide varying behavior depending on the density regime. On the basis of an extensive series of property calculations involving both molecules and solids, we show that this nonempirical methodology can lead to a balanced GGA description of both finite and extended systems.

DOI: 10.1103/PhysRevB.102.035129

I. INTRODUCTION

Even though the magnitude of the exchange and correlation contributions in Kohn-Sham density functional theory in general are small compared to the total energy of a many-electron system [1], approximations to those contributions determine the accuracy of calculated properties. Betterment of such approximations therefore is a continuing quest.

Those functionals depending solely on the electron density $n(\mathbf{r})$, and its gradient, through the dimensionless variable $s = |\nabla n(\mathbf{r})|/(2\,k_F\,n(\mathbf{r}))$, where $k_F = (3\pi^2 n)^{1/3}$, are called generalized gradient approximations (GGAs). They constitute the second rung of the so-called Jacob's ladder classification [2]. Their use has spread throughout the chemistry and condensed matter communities for the calculation of ground-state properties of atoms, molecules, solids, surfaces, and larger systems [3], not only due to the good balance between accuracy and computational effort when employed in periodic systems, but also because they are important ingredients in higher-rung functionals [4–6] and because they are the basis of the fourth-rung hybrid functionals widely used for thermodynamic properties of molecules [7].

Despite the popularity of GGAs, none of them so far has proved suitable for general use, unchanged, in *both* finite and periodic calculations or in simultaneous structural and energetic properties [8–14]. The issue is that their performance is limited by their dependence on a single set of fixed parameters. In nonempirical density functional approximations (DFAs), such parameters are designed to satisfy as many physical constraints as possible [15], consistent with reasonably simple expressions for the so-called enhancement function. For exchange, the enhancement function $F_x(s)$ is defined such that

$$E_x^{\mathrm{GGA}}[n] = \int d\mathbf{r}\, n(\mathbf{r}) \varepsilon_x^{\mathrm{unif}}(n) F_x(s), \tag{1}$$

where $\varepsilon_x^{\mathrm{unif}}(n)$ is the exchange energy per electron for the uniform electron gas of density $n(\mathbf{r})$. To recover the uniform electron gas limit, the exchange enhancement function must satisfy the second-order gradient expansion

$$F_x(s) \underset{s\to 0}{\longrightarrow} 1 + \mu s^2\ . \tag{2}$$

Critically, the coefficient $\mu = \mu_{\mathrm{GE}} = 10/81$, which is accurate for weakly inhomogeneous electron gases [16], has been shown to improve calculated lattice constants and bulk moduli of solids [9] when used in the Perdew-Burke-Ernzerhof (PBE) GGA form [17], a combination called PBEsol. However, that value of μ is not optimal for finite systems. Instead, $\mu = \mu_{\mathrm{MB}} \approx 0.219\,51$, the original PBE value, does better for atomization energies [17]. Any attempt to compute the properties of one system class with the parameter μ for the other class, and with $F_x(s)$ unchanged in Eq. (1), results in a rather poor performance [18].

The regularized gradient expansion functional [19], based on PBE, represents the first of several efforts that have been made to pursue a generally applicable GGA for atoms, molecules, and solids. This approximation keeps the value μ_{GE} fixed and restores the slowly varying limit for $s < 1$. Then its enhancement factor increases rapidly towards the same local Lieb-Oxford bound [20,21] as used in the PBE exchange functional. That increase is achieved through the addition of an s^4 term. A different scheme to satisfy the

*avela@cinvestav.mx

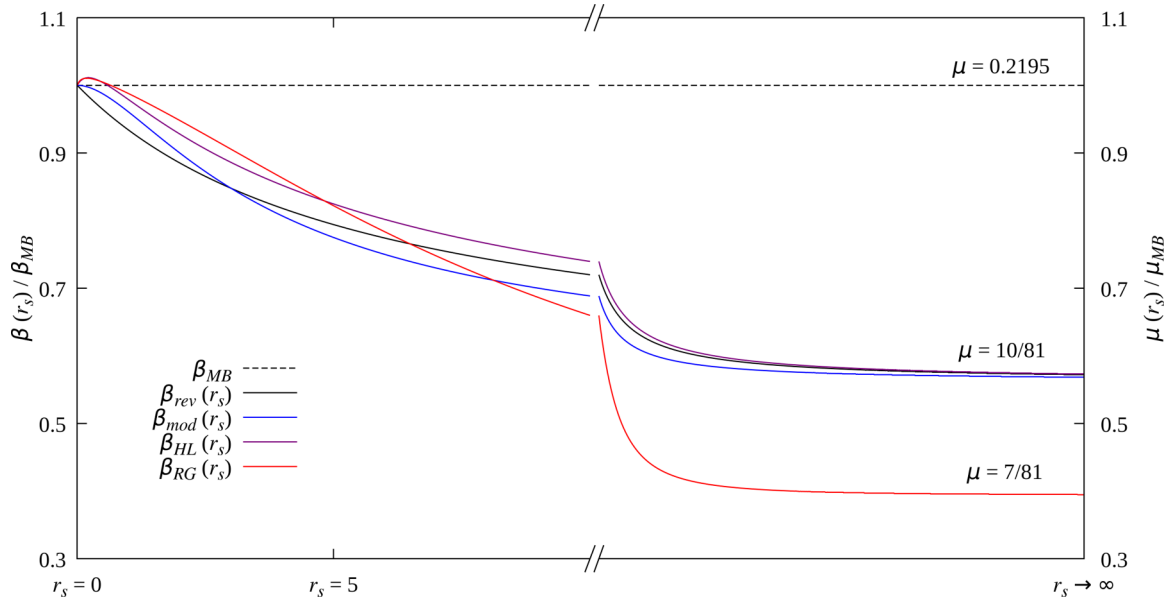

FIG. 1. Dependence of the correlation parameter β on the Wigner-Seitz radius r_s corresponding to the models described in the text and relative to the value from Eq. (3) that corresponds to $\mu = \mu_{\rm MB}$ used in PBE. The labels on the right indicate the low-density limits associated with the specified exchange parameter μ.

rapidly and slowly varying density limits also was explored [22]. In it the PBE form was retained and a sigmoid function was employed to interpolate from $\mu_{\rm GE}$ to $\mu_{\rm MB}$. Alternatively, $F_x(s)$ was expressed as a power-series expansion [23]. A fusion of two different functionals has been suggested as well [24].

Since the enhancement functions of all the aforementioned functionals still are based on a fixed set of parameters, their design remains intrinsically biased either toward solids and surfaces or toward atoms and molecules, a reason why they are frequently preferred to describe heterogeneous catalysis [25,26].

Motivated at least in part by the parametrization dilemma, nonseparable exchange-correlation DFAs also have been developed. The earliest consideration of nonseparable DFAs we have found is Ref. [27]. The separation of the exchange correlation energy $E_{\rm xc}$ into exchange and correlation terms can be justified as a convenient way to study and analyze the nature of those energy contributions. Thus, exchange can be defined as that part of an $E_{\rm xc}$ functional that scales linearly in the case of uniform density scaling, while correlation is the rest. It does not have simple scaling behavior [28,29]. The nonseparable idea reappeared in the late 1990s both as a specific form for DFA development [30–33] and as a discovered behavior of some extant DFAs [34]. It appears to have lain dormant until renewed interest and utilization by Truhlar and coworkers, mostly in the context of empirically parametrized DFAs [35–39].

Instead of focusing upon the slowly and rapidly varying limits, in the present work we explore a nonseparable parametrization approach based on the high- and low-density limiting behavior of the correlation energy of the weakly

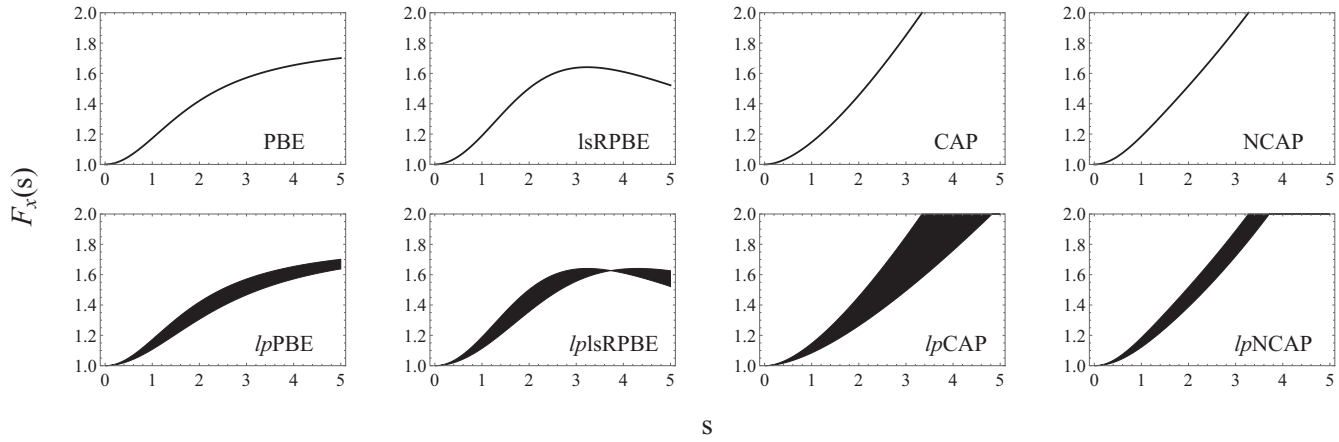

FIG. 2. Enhancement functions for several GGAs with a fixed $\mu = \mu_{\rm MB}$ (upper row) and their corresponding *lp*GGAs with the local parameter $\mu = \mu_{\rm rev}(r_s)$ (lower row) for the interval between $r_s \to 0$ and $r_s \to \infty$.

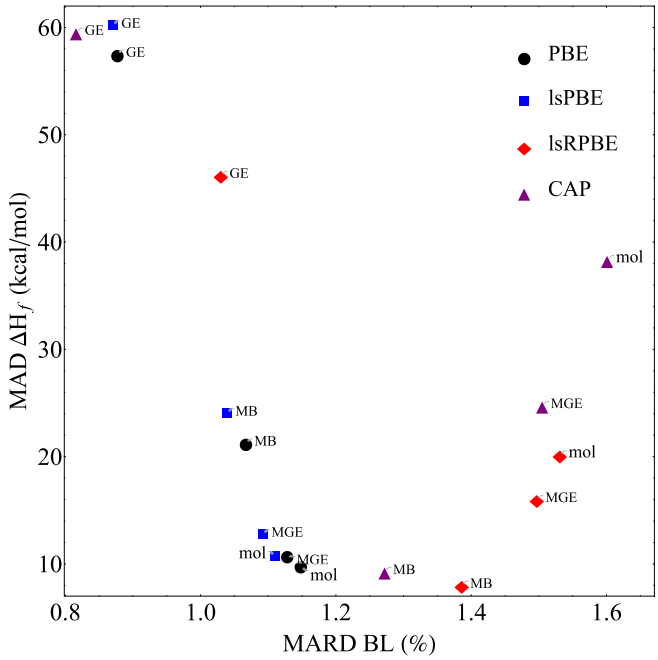

FIG. 3. Comparison of the mean absolute deviation for standard enthalpies of formation, ΔH_f, and the mean absolute relative deviation for bond lengths, BL, using different fixed values of μ_x, with $x = \{\text{GE, MB, MGE, mol}\}$, which are ordered in increasing value of μ_x.

inhomogeneous electron gas. Doing so provides an additional degree of freedom to the exchange enhancement function through the local density dependence of the second-order coefficient μ from the correlation gradient expansion. That density-dependent relationship between coefficients is what introduces the nonseparability in a DFA form that otherwise would be separable. We apply this methodology to various DFAs on several sets of molecules and solids to provide a performance overview with respect to earlier GGAs.

II. FUNCTIONAL CONSTRUCTION

A. Limiting behaviors

In the exchange PBE functional, the value of μ modulates the weight given to density gradients in the exchange energy and provides control over $F_x(s)$ both for slowly varying densities, $s \to 0$, and for the case $s \to \infty$. The latter situation can correspond to rapidly varying density but also applies, ambiguously, to the case of asymptotically small, smooth densities. For correlation, PBE uses a parameter β to control the effects of density variation. The two parameters are related in PBE by the choice

$$\mu = \frac{\pi^2}{3}\beta, \tag{3}$$

in order to recover the linear response of the uniform electron gas. This specific assumption has been used recently in designing global hybrids [40], long-range screened hybrids [41], and short-range screened hybrids [42].

This fixed parametrization omits a density dependence. The gradient expansion of the correlation contribution begins as

$$E_c[n] = \int d\mathbf{r}\, n(\mathbf{r})\left[\varepsilon_c^{\text{unif}}(n) + \beta_c(n)t^2 + \dots\right], \tag{4}$$

where $\varepsilon_c^{\text{unif}}(n)$ is the correlation energy per particle of the uniform electron gas, and $t = |\nabla n|/[4(3/\pi)^{1/6}n^{7/6}]$. The coefficient $\beta_c(n)$ usually is expressed in terms of the dimensionless Wigner-Seitz radius r_s as $\beta_c(r_s) = 16(3/\pi)^{1/3}C_c(r_s)$,

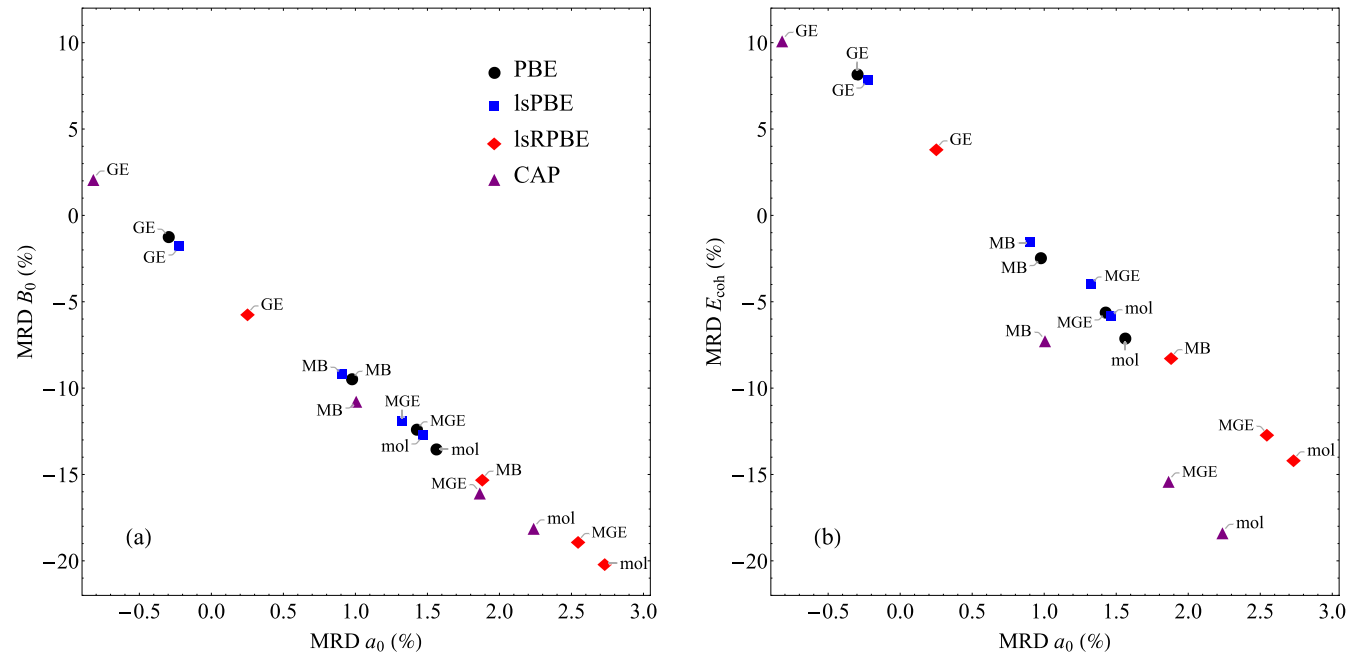

FIG. 4. Mean relative deviations of the bulk modulus and cohesive energies versus the lattice constants using the different values $x = \{\text{GE, MB, MGE, mol}\}$ for μ_x, ordered by increasing magnitude.

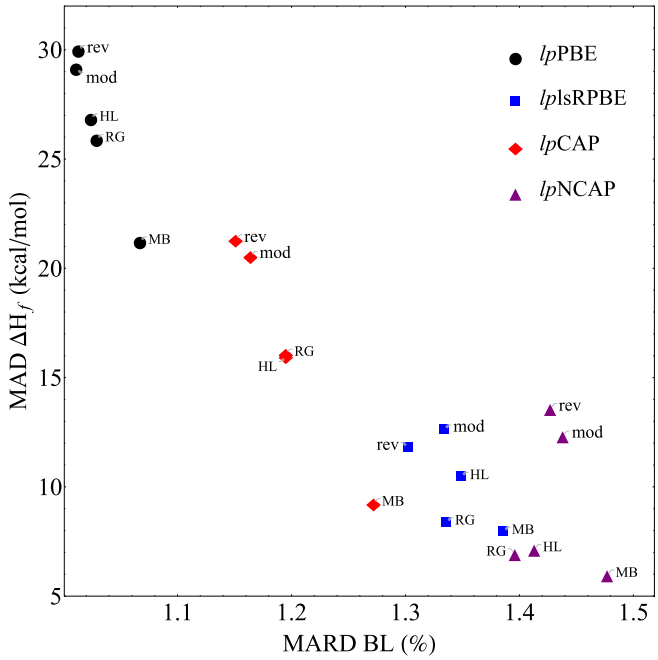

FIG. 5. MAD for ΔH_f versus MARD for bond lengths, BL, for *lp*GGAs using the set $\mu_x(r_s)$ for exchange and $\beta_x(r_s)$ for correlation, with $x = \{\text{MB, rev, mod, HL, RG}\}$.

where $r_s = [3/(4\pi n)]^{1/3} {B_0}^{-1}$, and $B_0 = 1$ is the Bohr radius in atomic units. For $n(\mathbf{r}) \to \infty$, Ma and Brueckner [43] demonstrated that

$$\lim_{n\to\infty} \beta_c = \beta_{\text{MB}} = 16(3/\pi)^{1/3} C_c(0) \approx 1.975\,63/3\pi^2 = 0.066\,724\,4\,. \quad (5)$$

This result, if substituted in Eq. (3), gives rise to the value μ_{MB} already quoted. Shortly thereafter, Rasolt and Geldart [44], independently of Hu and Langreth [45], included the local density dependence of Eq. (5) [46]. Rasolt and Geldart derived an analytic representation for $C_c(r_s)$. Later this was employed for the construction of the P86 correlation parametrization [47], with the form

$$C_{\text{RG}}(r_s) = c_1 + \frac{c_2 + c_3\, r_s + c_4\, r_s^2}{1 + c_5\, r_s + c_6\, r_s^2 + c_7\, r_s^3}, \quad (6)$$

where $c_1 = 0.001\,667$, $c_2 = 0.002\,568$, $c_3 = 0.023\,266$, $c_4 = 7.389 \times 10^{-6}$, $c_5 = 8.723$, $c_6 = 0.472$, and $c_7 = 7.389 \times 10^{-2}$. The results that Hu and Langreth obtained beyond the random phase approximation were expressed roughly by

$$\beta_{\text{rev}}(r_s) = \beta_{\text{MB}} \frac{1 + c_1\, r_s}{1 + c_2\, r_s}, \quad (7)$$

with the values $c_1 = 0.1$ and $c_2 = 0.177\,8$ employed in the construction of the revTPSS correlation functional [48]. However, recently it was shown that more refined inclusion of r_s dependence in the Padé approximant can lead to an improved correction. Hence, two more approximants were devised [49]. Both share the form

$$\beta_{\text{mod/HL}}(r_s) = \beta_{\text{MB}} \frac{1 + c_1\, r_s(c_2 + c_3\, r_s)}{1 + c_1\, r_s(1 + c_4\, r_s)}\,. \quad (8)$$

Two parameter sets were proposed. The set $c_1 = 1/2$, $c_2 = 1$, $c_3 = 1/6$, and $c_4 = 0.296\,33$ is used for $\beta_{\text{mod}}(r_s)$ in order to have a slope equal to 0 when $r_s \to 0$. The second set has $c_1 = 3$, $c_2 = 1.046$, $c_3 = 0.1$, and $c_4 = 0.177\,8$ in $\beta_{\text{HL}}(r_s)$ to recover the positive slope of the original Hu and Langreth form.

By design, Eqs. (7) and (8) were chosen so that

$$\beta(r_s) \xrightarrow[r_s\to 0]{} \beta_{\text{MB}}, \quad (9)$$

$$\beta(r_s) \xrightarrow[r_s\to\infty]{} \beta_{\text{GE}}, \quad (10)$$

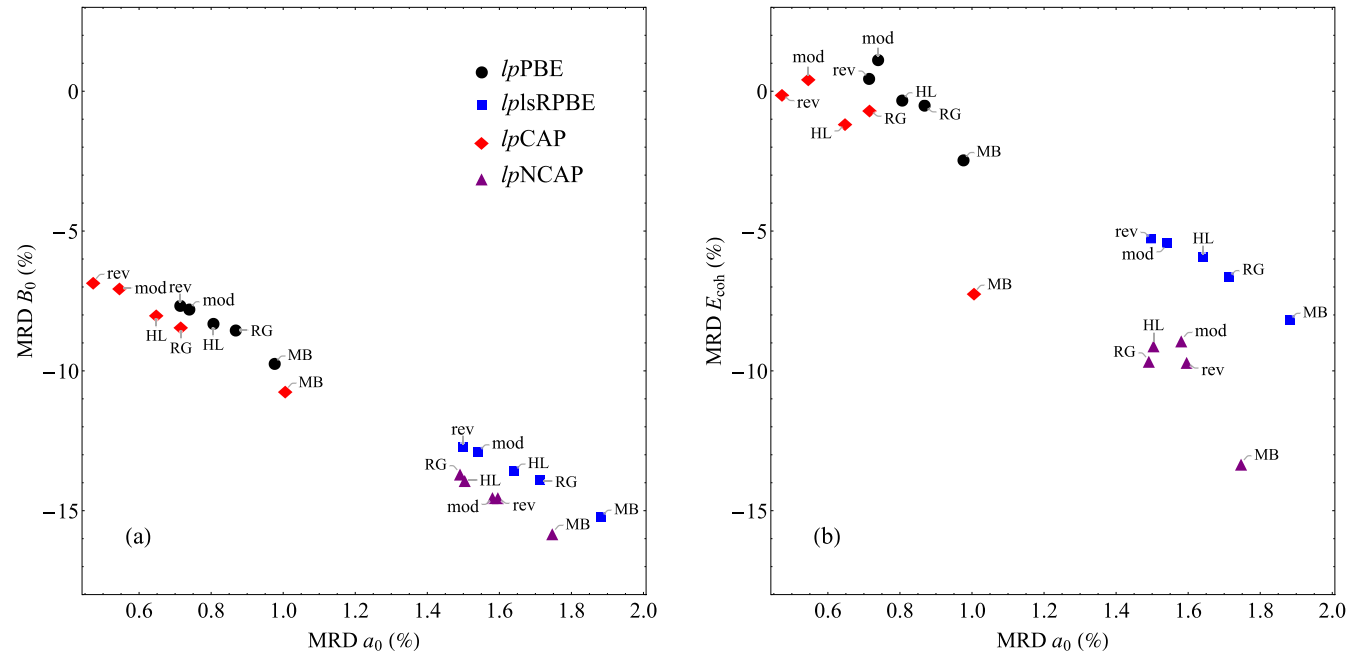

FIG. 6. MRD of B_0 and E_{coh} versus a_0 using the set $\mu_x(r_s)$ for exchange and $\beta_x(r_s)$ for correlation, with $x = \{\text{MB, rev, mod, HL, RG}\}$.

where $\beta_{\rm GE} = 10/(27\pi^2) = 0.037\,526$ is the second-order correlation coefficient for slowly varying densities. It is noteworthy that $\beta_{\rm RG}(r_s)$ has the same limiting behavior as Eq. (9), but a different value for the low-density limit, (10). Further substitution of $\beta_{\rm rev}(r_s)$, $\beta_{\rm mod}(r_s)$, $\beta_{\rm HL}(r_s)$, and $\beta_{\rm RG}(r_s)$ in Eq. (3) delivers four different, density-dependent values for the second-order coefficient for exchange, namely, $\mu_{\rm rev}(r_s)$, $\mu_{\rm mod}(r_s)$, $\mu_{\rm HL}(r_s)$, and $\mu_{\rm RG}(r_s)$. All of them have limiting conditions analogous to those for the $\beta(r_s)$ correlation coefficient,

$$\mu(r_s) \xrightarrow[r_s\to 0]{} \mu_{\rm MB}, \tag{11}$$

$$\mu(r_s) \xrightarrow[r_s\to\infty]{} \mu_{\rm GE}\ . \tag{12}$$

The sole exception is $\mu_{\rm RG}(r_s) \approx 7/81$ for $r_s \to \infty$, which corresponds to Sham's coefficient [50]. We include it for general utility in functional construction despite the fact that it is known to be incorrect. A plot of the $\beta(r_s)$ functions discussed above as a function of r_s is shown in Fig. 1.

B. Implementation

Once the dependence on $n(\mathbf{r})$ has been included in what formally is the exchange contribution via $\mu(r_s)$, we can construct or select enhancement factors that interpolate reasonably between the values defined by the high- and low-density limits of the previously described approximants. It is important to note that although the enhancement factors under consideration were constructed and constrained as separable forms, the local parametrization prescription just described makes the resulting DFA nonseparable. For example, the introduction of a density-dependent μ via the density-dependent β means that what formally was an exchange energy no longer obeys uniform scaling for exchange [28,29].

The implementation of this methodology is quite straightforward. Here we have selected four nonempirical GGA exchange functionals in which to include the different $\mu(r_s)$ values. These are the widely used PBE [17]; lsRPBE [51], which is designed to satisfy the large dimensionless gradient decay [21]; CAP [52], which forces $F_x(s)$ to diverge as $s \to \infty$ and includes the correct asymptotic potential [53]; and, finally, NCAP [54], whose performance on standard thermochemistry sets is comparable to higher-rung approximations. For correlation, we included the set of $\beta(r_s)$ and $C(r_s)$ for PBE and P86, respectively (see Sec. II of the Supplemental Material [55]).

We denote these functionals *lp*PBE, *lp*lsRPBE, *lp*CAP, and *lp*NCAP, or collectively *lp*GGAs, where *lp* stands for local parameter. Their exchange enhancement factors are

$$F_x^{lp\rm PBE}(s) = 1 + \kappa - \frac{\kappa}{1 + \frac{\mu(r_s)}{\kappa} s^2}, \tag{13}$$

$$F_x^{lp\rm lsRPBE}(s) = 1 + \kappa - \kappa\, e^{-\frac{\mu(r_s)}{\kappa} s^2} - (1+\kappa)\left(1 - e^{-\alpha \frac{\mu(r_s)}{\kappa} s^2}\right), \tag{14}$$

$$F_x^{lp\rm CAP}(s) = 1 + \mu(r_s) \frac{s \ln[1+s]}{1 + c\,\mu(r_s) \ln[1+s]}, \tag{15}$$

$$F_x^{lp\rm NCAP} = 1 + \mu(r_s) \tanh[s] \sinh^{-1}[s] \times \frac{1 + \frac{\gamma}{c\,\mu(r_s)}\{(1-\zeta) s \ln[1+s] + \zeta\, s\}}{1 + \gamma \tanh[s] \sinh^{-1}[s]}, \tag{16}$$

where $\kappa = 0.804$, $\alpha = 0.023\,534$, $c = 3/(4\pi)$, $\gamma = 0.018\,086$, and $\zeta = 0.304\,121$. It should be noted that the values of ζ and γ correspond to the case for which μ is a constant, fixed at the PBE value, i.e., $\mu_{\rm MB}$. In principle, both ζ and γ should be parameters that correspond to the local $\mu(r_s)$ but these effects are expected to be small compared to the effects of the local μ itself. The notation F_x is used *solely* to indicate the parentage of these enhancement factors. We iterate that in this form they are not pure exchange. A comparison of Eqs. (13) to (16) for the fixed value $\mu_{\rm MB}$ and the local parameter $\mu_{\rm rev}(r_s)$, depicted in Fig. 2, shows how the local dependence on $n(\mathbf{r})$ produces more versatile enhancement functions. Notably, their shapes can vary inside the black regions, unlike those approximations with fixed parameter sets illustrated in the first row of panels in Fig. 2.

III. RESULTS AND DISCUSSION

Calculations on molecules were done with a developmental version of NWChem 6.6 [56], using the same test sets of molecules and computational parameter choices as in Ref. [57], while computations for solids were performed with a modified version of VASP [58–60]. We used the same crystalline test data sets for periodic systems as in Ref. [6], except that we omitted Y due to convergence issues with CAP and NCAP. Moreover, there were two minor changes in computational details. For all compounds involving Li, the cutoff was increased to 1200 eV, and approximate isolated atom energies were calculated with an $11 \times 12 \times 13$ Å^3 cell.

For the sake of thorough context, we first analyze the effect of different fixed values of μ on molecules and solids. In addition to $\mu_{\rm GE}$ and $\mu_{\rm MB}$, two other nonempirical values have been reported in the literature. These are $\mu_{\rm MGE} = 0.26$, obtained from the asymptotic expansion of the semiclassical neutral atom [61], and $\mu_{\rm mol} = 0.275\,83$, from the self-interaction cancellation for the hydrogen atom [57].

To begin, Fig. 3 depicts the effect for molecules of the four choices of fixed μ on the behavior of the mean absolute deviation (MAD) for the standard enthalpies of formation and mean absolute (unsigned) relative deviation (MARD) of the bond lengths. Here we have included lsPBE [51] (same as lsRPBE but with a PBE kernel instead) in lieu of NCAP in order to classify the functionals in two distinct groups, one for the enhancement functions of PBE and lsPBE and the other for lsRPBE and CAP. There are two main messages in Fig. 3. The first, long known, is that independently of the form of $F_x(s)$, an increase in μ is accompanied by a loss in structural description accuracy. The second message is related more to thermodynamic values. Functionals such as lsRPBE and CAP reach their optimum performance for both properties with a value of μ smaller than those such as PBE and lsPBE. That optimum value is generally $\mu_{\rm MB}$, above which the thermodynamic accuracy deteriorates. The underpinnings

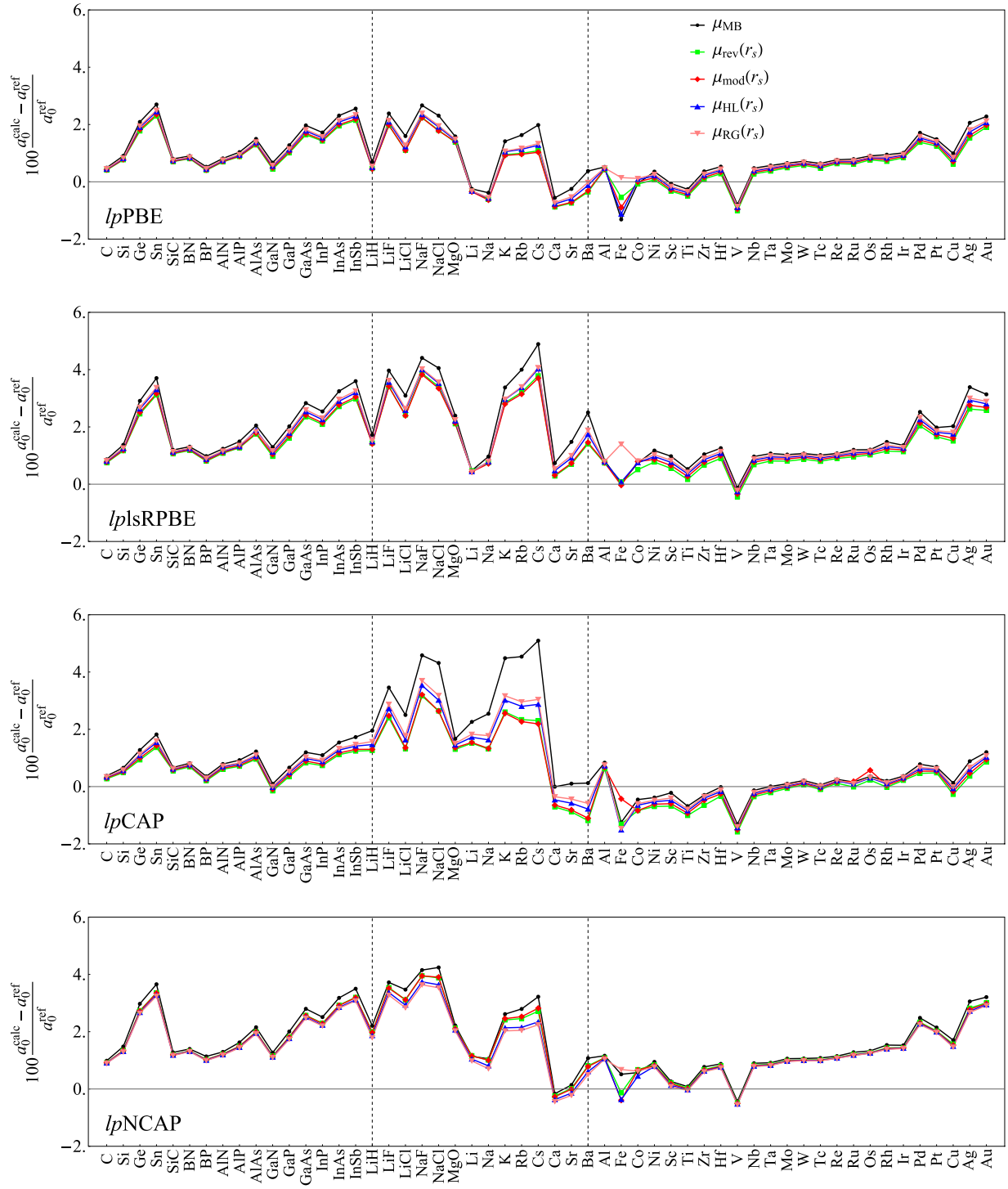

FIG. 7. Relative deviation of lattice constants for the solids considered in this work. The *lp*GGAs use the set $\mu_x(r_s)$ for exchange and $\beta_x(r_s)$ for correlation, with $x = \{\mathrm{MB}, \mathrm{rev}, \mathrm{mod}, \mathrm{HL}, \mathrm{RG}\}$.

of this behavior are atomic. The smaller the μ value is, the more underestimated are the energies of the atoms, hence, energy differences between molecules and atoms are more overestimated with μ_{GE} and somewhat underestimated with μ_{mol} for lsRPBE and CAP.

Among the most obvious properties of interest in solids are the lattice constants, a_0, bulk modulus, B_0, and cohesive energies, E_{coh}. Figure 4(a) shows that whenever the mean relative deviation (MRD) of the lattice constants increases, the bulk modulus MRD does the opposite in an almost-linear response to the value of μ. Conversely, Fig. 4(b) shows that cohesive energies go from overestimates to underestimates as μ is increased, in accordance with the behavior observed for molecules in Fig. 3 for the formation enthalpies. Further

comparison in Fig. 4 reveals that for a balanced description of a_0, B_0, and $E_{\rm coh}$, the interval of interest of μ_x lies between $\mu_{\rm GE}$ and $\mu_{\rm MB}$, corresponding to the limits in Eqs. (11) and (12) used for the construction of $\mu(r_s)$.

Now we turn to the *lp*GGAs. We observed that *lp*PBE, *lp*lsRPBE, and *lp*CAP perform better when combined with the PBE correlation, while *lp*NCAP is better with P86 correlation. Hence, the following discussion is for those combinations. Figure 5 depicts how the MAD for ΔH_f is worsened with respect to the functionals with fixed parameters identified with the label MB. This disadvantage is more evident for *lp*CAP than for the rest of the functionals. Nevertheless, this behavior is expected due to the limits imposed in the Padé approximants for both exchange and correlation. In this respect it should also be highlighted that the consequence of these limits is to underestimate more the total energies of atoms in comparison to the molecules, with the overall result of overestimating ΔH_f, but this overestimation is at least 50 % smaller compared to the fixed value $\mu_{\rm GE}$ (see Fig. 3).

Bond lengths, onthe other hand, exhibit trends opposite to enthalpies of formation. The addition of r_s dependence in the second-order coefficients of Eq. (3) lowers the rate at which the enhancement functions grow, because r_s reduces the weight given to the density gradients in the exchange and correlation functionals. Thus, it favors the structural description of molecules compared to the magnitude of the deviations obtained keeping $\mu = \mu_{\rm MB}$ and $\beta = \beta_{\rm MB}$ fixed. We can also observe in Fig. 5 that except for *lp*NCAP, the *lp*GGAs using $\mu_{\rm HL}(r_s)$ and $\mu_{\rm RG}(r_s)$ produce larger errors in the bond lengths than $\mu_{\rm rev}(r_s)$ and $\mu_{\rm mod}(r_s)$, probably due to the maxima shown in the $\beta(r_s)$ function located at small values of r_s. It is also noteworthy that the data depicted in Fig. 5 does not allow recommending a general choice of $\mu(r_s)$. Instead, we observe different trends for each functional. Overall, for all the *lp*GGAs considered, the local dependence on $\mu(r_s)$ improves the description of bond distances but at the expense of degrading the quality of the heats of formation.

It should be noted that GGA functionals with fixed parameters such as PBE and lsPBE provide better performance for heats of formation and bond lengths (see black circles and blue squares labeled "MGE" and "mol" at the bottom of Fig. 3) than the lpGGAs depicted in Fig. 5. Nonetheless, when considered in the context of balanced performance on both molecules and condensed phases (see below) from a single DFA, it can be concluded that the functionals *lp*lsRPBE and *lp*NCAP, combined with $\mu_{\rm RG}(r_s)$, provide acceptable predictions of structural and thermodynamic data for molecules. By selecting the MAD for ΔH_f and MARD for bond lengths in the axes in Figs. 3 and 5 one obtains scales from which the effects of DFAs and of the μ_x parameter are clearer than from the use of other combinations of statistical deviations. Values for the MAD, MD, and MARD are listed in the tables in Sec. III of the Supplemental Material [55].

Turning to the results for extended systems, the first thing to note in Fig. 6(a) is that there is a clustering of the results provided by *lp*PBE and *lp*CAP, on one hand, and *lp*lsRPBE and *lp*NCAP, on the other. The former functionals show a better performance in lattice constants and bulk modulus than the latter. Also, it is clear in Fig. 6(a) that including the local behavior in μ_x reduces the deviations in the bulk modulus and

TABLE I. Mean absolute deviations for standard enthalpies of formation (G3), ionization potentials (IPs), electron affinities (EAs), proton affinities (PAs), bond length (BLs), binding energies (BEs), barrier heights of forward nonhydrogen transfer (NHBH-f), reverse nonhydrogen transfer (NHBH-r), forward hydrogen transfer (HBH-f), reverse hydrogen transfer (HBH-r), lattice constants (a_0), bulk moduli (B_0), and cohesive energies ($E_{\rm coh}$). Units are expressed as follows: G3, IP, EA, PA, BE, NHBH-f, NHBH-r, HBH-f, and HBH-r, in kcal/mol; BL and a_0, in Å; B_0 in GPa; and $E_{\rm coh}$, in eV/atom. For clarity, see text regarding the X and C designations.

	X	NCAP	lsRPBE	CAP	PBE	*lp*CAP	RGE2	PBEint	PBEsol
Property	C	P86	PBE	PBE	PBE	PBE	PBE	PBE	PBE
G3		5.97 ± 0.35	7.93 ± 0.43	9.23 ± 0.49	21.21 ± 1.00	15.97 ± 0.78	30.19 ± 1.28	40.23 ± 1.70	57.44 ± 2.42
G3/atom		1.27	1.43	1.62	3.19	2.59	4.24	5.44	7.52
G3/electron		0.23	0.26	0.30	0.63	0.48	0.86	1.14	1.62
IP		4.00 ± 0.92	3.30 ± 0.78	2.55 ± 0.53	3.47 ± 0.85	2.52 ± 0.52	2.26 ± 0.45	2.33 ± 0.47	2.63 ± 0.56
EA		3.70 ± 1.05	2.60 ± 1.05	3.65 ± 0.56	2.64 ± 0.98	3.52 ± 0.53	2.45 ± 0.66	2.33 ± 0.69	2.63 ± 0.72
PA		1.32 ± 0.52	1.22 ± 0.37	1.53 ± 0.53	1.39 ± 0.32	1.27 ± 0.47	1.86 ± 0.38	2.27 ± 0.38	2.87 ± 0.52
BL		0.0236 ± 0.0001	0.0219 ± 0.0001	0.0205 ± 0.002	0.0163 ± 0.0001	0.0190 ± 0.002	0.0189 ± 0.0001	0.0167 ± 0.0001	0.0131 ± 0.0001
BE		2.39 ± 0.39	1.53 ± 0.29	2.70 ± 0.42	1.64 ± 0.34	1.91 ± 0.37	1.60 ± 0.35	1.78 ± 0.36	2.25 ± 0.41
NHBH-f		9.39 ± 1.60	9.76 ± 1.71	8.22 ± 1.79	10.38 ± 1.67	9.34 ± 1.70	10.35 ± 1.61	10.85 ± 1.58	11.69 ± 1.54
NHBH-r		8.71 ± 1.53	9.44 ± 1.62	7.99 ± 1.71	9.96 ± 1.78	8.88 ± 1.79	9.66 ± 1.94	10.09 ± 2.03	10.76 ± 2.21
HBH-f		6.80 ± 0.75	7.76 ± 0.81	6.92 ± 0.76	9.49 ± 0.96	8.60 ± 0.82	10.45 ± 0.93	11.40 ± 1.02	13.05 ± 1.16
HBH-r		6.98 ± 0.76	8.25 ± 0.69	7.11 ± 0.63	9.72 ± 0.73	8.82 ± 0.67	10.52 ± 0.76	11.38 ± 0.82	12.82 ± 0.93
a_0		0.083 ± 0.009	0.089 ± 0.010	0.057 ± 0.010	0.053 ± 0.006	0.045 ± 0.006	0.044 ± 0.007	0.035 ± 0.004	0.028 ± 0.004
B_0		18.028 ± 2.27	17.863 ± 2.31	9.939 ± 1.36	12.238 ± 1.70	9.234 ± 1.27	9.359 ± 1.30	8.471 ± 1.23	8.025 ± 1.41
$E_{\rm coh}$		0.513 ± 0.04	0.420 ± 0.04	0.354 ± 0.04	0.220 ± 0.03	0.303 ± 0.04	0.273 ± 0.04	0.300 ± 0.05	0.435 ± 0.06

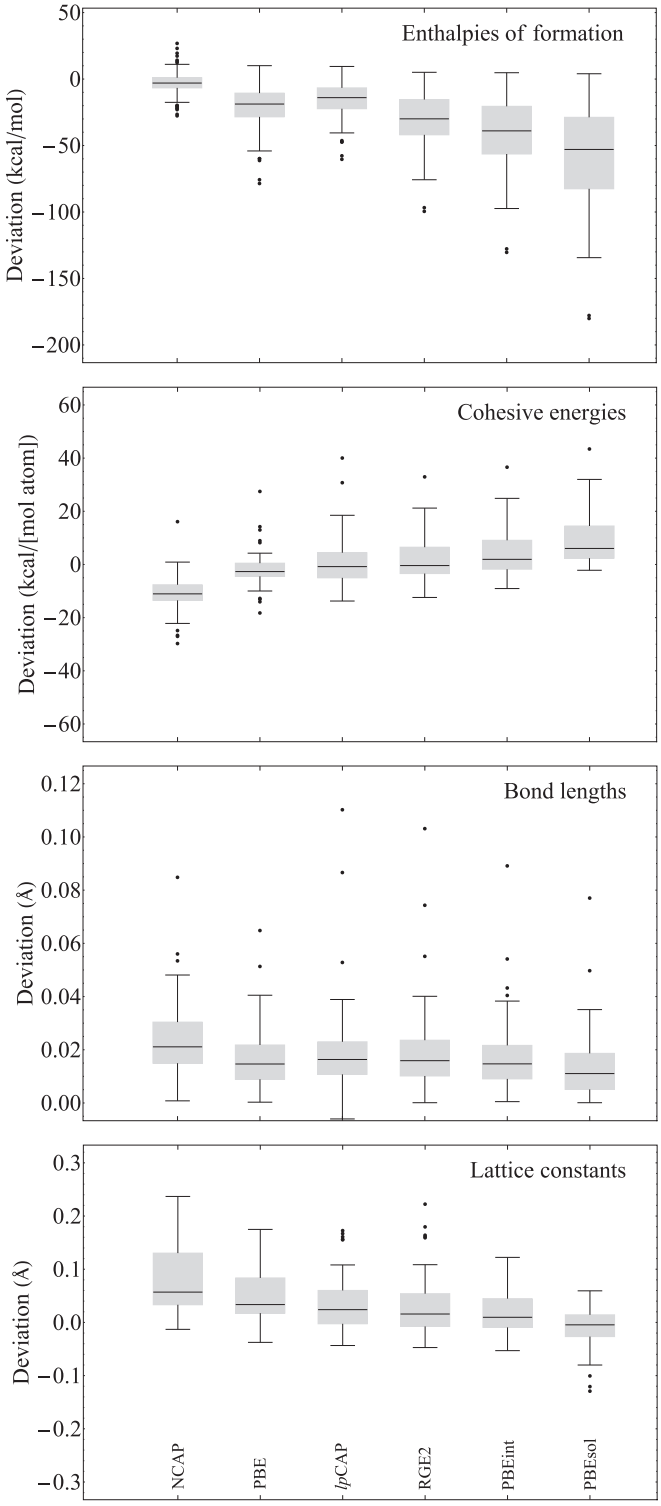

FIG. 8. Box plots of different properties for a representative set of functionals. See text for explanation.

lattice constants of solids. Therefore, it seems to be generally valid that *lp*GGAs provide better predictions for the mechanical properties of solids. The results for the cohesive energies show a similar clustering of functionals, as shown in Fig. 6(b). From the two plots depicted in Fig. 6 one can conclude that the *lp*PBE and *lp*CAP functionals combined with $\mu_{\rm rev}(r_s)$ are the best *lp*GGAs to be used in extended systems. These results indicate that local parameters in nonseparable exchange-correlation GGAs can provide a better balance between finite and extended systems. The clustering and behavior shown in Figs. 4 and 6 are better defined when using the MRDs for the solid properties. The scales provided by other statistical deviations do not show this clean distinction.

In a recent study on a large set of density functional approximations from different rungs of Jacob's ladder, Tran, Stelzl, and Blaha [62] showed that an inappropriate shape of the enhancement function makes many approximations fail in the description of a_0, B_0, and $E_{\rm coh}$, particularly for alkali and alkali-earth metals. So to obtain deeper insight into the performance of *lp*GGAs over the entire set of extended systems, in Fig. 7 we plot the relative deviation for every solid and functional. As expected, the major differences in *lp*GGAs come from alkali and alkali-earth metals. These results are shown between the dashed vertical lines in Fig. 7. Taking as the starting point the original functional with the fixed parameter $\mu_{\rm MB}$, PBE shows the smallest deviations for these systems, while CAP delivers the largest, followed closely by lsRPBE and NCAP.

The rationale for these deviations in alkali metals relies on the values of the dimensionless gradient ($s > 1$) in the core-valence separation region [63]. In the latter work it also was noted that for these solids r_s has a moderately near-constant value in the interstitial region that arises from the overlap of diffuse valence-electron densities. Hence it was argued that this makes a nonnegligible contribution to the derivatives of both the exchange and the correlation approximations.

Since $F_x(s)$ in *lp*GGAs also depends on r_s, a higher value of r_s weakens the enhancement function [see Eq. (12)], and as a result it contributes to ameliorating, in part, the artificial overestimation of a_0 for alkali metals. Figure 7 shows how *lp*GGAs in general reduce the relative error of lattice constants for the whole set, with a greater effect upon alkali and alkali-earth materials than the others. Even though *lp*PBE, *lp*lsRPBE, and *lp*NCAP do not show an improvement as strong as *lp*CAP does, it is enough to reduce the mean relative deviation depicted in Fig. 6.

Along with these last results it is appropriate to mention that PBE also has proven to be one of the most successful approximations for the calculation of lattice constants for transition metals [64–66]. In Fig. 7 we observe how the *lp*PBE family is comparatively better than *lp*lsRPBE and *lp*NCAP, whose relative deviations are systematically larger. Nevertheless, we cannot disregard the fact that the *lp*CAP family is as competitive as *lp*PBE for these materials and in some cases it outperforms the latter.

In Table I we gather the mean absolute deviations and their uncertainties [67] for a set of properties important for chemistry and materials physics as generated by a representative selection of GGAs. They may be divided into three groups. From left to right, the first group is composed of NCAP, lsRPBE, CAP, and PBE, designed for molecules. Then there are *lp*CAP using $\mu_{\rm HL}(r_s)$, RGE2 [19], and PBEint [22], aimed at describing molecules and solids. Finally, PBEsol [9] is specifically calibrated for bulk solid calculations. The

headings "X" and "C" in Table I denote the exchange and correlation functionals, respectively. Obviously in the case of the nonseparable lpGGAs, that labeling refers to the parent functional, not its role in the *lp* combination. (Complete lists corresponding to Table I comparing popular separable functionals with locally parametrized variants are included in the Supplemental Material [55].) From the results in Table I it becomes clear that whatever works best for molecules does the opposite for solids, and vice versa. For instance, standard enthalpies of formation are well described with the first group of functionals and poorly described with PBEsol, yet that functional is itself very accurate for lattice constants and bulk modulus, while the first group is not. This observation is consistent with earlier findings summarized in Sec. I.

Then halfway in Table I are the intermediate approximations that provide compromises between molecules and periodic systems. One sees that RGE2 and PBEint still favor solids. Even though they remain accurate for a_0, B_0, and $E_{\rm coh}$, their performance for the thermochemistry set G3 is at least 9 kcal/mol larger than for PBE. This is not the case for *lp*CAP with the local dependence $\mu_{\rm HL}(r_s)$ in what nominally is exchange and $\beta_{\rm HL}(r_s)$ for what nominally is correlation. This provides advantages of approximately 47% versus RGE2 and about 60% versus PBEint for this same property. Moreover, *lp*CAP competes very closely with RGE2 for lattice constants and bulk modulus, while at the same time it performs as well as PBEint for cohesive energies. The rest of the properties are approximately equally well described, with subtle differences.

With respect to the other functionals, *lp*CAP outperforms NCAP, lsRPBE, CAP, and PBE for a_0 and B_0, but PBE is better for $E_{\rm coh}$. The latter statement is notwithstanding the fact that PBEsol remains the best functional for a_0 and B_0.

Using the data in Table I, additional statistical analyses of representative functionals and properties were done. The results are depicted as box plots in Fig. 8. In this analysis, the signed deviations $P_{\rm calc} - P_{\rm ref}$ for property P are used to generate the boxes corresponding to the interquartile range, with the minimum and maximum deviations shown by the end of the whiskers. The black horizontal line indicates the median value and the outliers in the set are depicted by the dots. The median corresponds to the mean (signed) deviation [67]. In general, as we move from the functionals designed for molecules to those designed for periodic systems, we can verify that the error distributions for the enthalpies of formation and cohesive energies become wider. In contrast, for bond lengths and lattice constants the error distributions narrow. Also noticeable are the opposite trends exhibited by the median values of the energetic properties for molecules and solids, while the structural description is practically the same for both kind of systems, although bond lengths are overestimated whereas lattice constants also include underestimated values.

Finally, we did not consider whether layered solids such as graphite and hexagonal boron nitride are well treated, nor did we consider Kohn-Sham bandgaps for semiconductors or insulators. The layered systems are known to be bound mainly by weak interactions, hence dispersion corrections are needed in order to describe them appropriately [62]. Regarding bandgaps, the omitted functional derivative discontinuity of the energy with respect to the electron density in the exchange and correlation functionals under consideration, except for lpNCAP, makes any bandgap calculation an underestimate by as much as a factor of 2 [68,69]. However, NCAP and, therefore, lpNCAP introduce the derivative discontinuity effects through the asymptotic behavior of the exchange correlation potential. Thus, it will be worthwhile to analyze the performance of NCAP and lpNCAP in the prediction of bandgaps.

IV. CONCLUDING REMARKS

The study presented here reveals that conversion of GGAs to a nonseparable form by the use of local parameters $\mu(r_s)$ and $\beta(r_s)$ in what originally were the exchange and correlation contributions, respectively, adds enough flexibility to account for roughly equal treatment of molecules and solids without adding computational effort. Moreover, these nonempirical nonseparable GGAs with local parameters can fulfill the two different values of the second-order coefficient from the gradient expansion, namely, that of Ma and Brueckner for the high-density limit and that of Antoniewicz and Kleinman for the low-density limit.

Results for molecules showed that these local parameters reduce the errors on calculated bond lengths and that the thermodynamic description with these functionals is at least 45% less in error in comparison to other nonempirical approximations that pursue a balanced description of finite and extended systems as well. Meanwhile for solids, a detailed analysis of the calculated lattice constants revealed that this nonempirical parametrization also is capable of circumventing the problems associated with alkali and alkali-earth metals, for which the local parameters correctly reduce the overestimation of what formally are the exchange and correlation energies. We additionally showed that bulk moduli and cohesive energies are more appropriately described when we added the local parameters to several density functional approximations.

Overall, due to the flexibility that the enhancement functions can acquire, this scheme is a promising alternative to explore further in the design of new generalized gradient approximations for the exchange-correlation energy.

ACKNOWLEDGMENTS

A.A.-M. is grateful for partial financial support by the University of Florida through Project No. 00043841 and Conacyt through project Fronteras 867. S.B.T. was supported in part by US National Science Foundation Grant No. DMR-1515307 and, for the latter part of the work, US Department of Energy Grant No. DE-SC 0002139. J.L.G. thanks Conacyt for Grant No. 237045, and A.V. for grant Fronteras 867. All calculations were done on HiPerGator at University of Florida and on the computational facilities of the Department of Chemistry in Cinvestav.

[1] W. Kohn and L. J. Sham, Phys. Rev. **140**, A1133 (1965).

[2] J. P. Perdew and K. Schmidt, in *Density Functional Theory and Its Application to Materials*, edited by V. Van Doren, C. Van Alsenov, and P. Geerlings (AIP, Melville, NY, 2001).

[3] *A Primer in Density Functional Theory*, edited by C. Fiolhais, F. Nogueira, and M. Marques (Springer-Verlag, New York, 2003).

[4] J. Sun, A. Ruzsinszky, and J. P. Perdew, Phys. Rev. Lett. **115**, 036402 (2015).

[5] D. Mejía-Rodríguez and S. B. Trickey, Phys. Rev. A **96**, 052512 (2017).

[6] D. Mejía-Rodríguez and S. B. Trickey, Phys. Rev. B **98**, 115161 (2018).

[7] E. Fabiano, L. A. Constantin, and F. J. Della Sala, J. Chem. Theory Comput. **7**, 3548 (2011).

[8] J. P. Perdew, K. Burke, and M. Ernzerhof, Phys. Rev. Lett. **80**, 891 (1998).

[9] J. P. Perdew, A. Ruzsinszky, G. I. Csonka, O. A. Vydrov, G. E. Scuseria, L. A. Constantin, X. Zhou, and K. Burke, Phys. Rev. Lett. **100**, 136406 (2008).

[10] Y. Zhao and D. G. Truhlar, J. Chem. Phys. **128**, 184109 (2008).

[11] J. P. Perdew, A. Ruzsinszky, G. I. Csonka, O. A. Vydrov, G. E. Scuseria, L. A. Constantin, X. Zhou, and K. Burke, Phys. Rev. Lett. **102**, 039902(E) (2009).

[12] G. I. Csonka, J. P. Perdew, A. Ruzsinszky, P. H. T. Philipsen, S. Lebegue, J. Paier, O. A. Vydrov, and J. G. Ángyán, Phys. Rev. B **79**, 155107 (2009).

[13] P. Haas, F. Tran, P. Blaha, L. S. Pedroza, A. J. R. da Silva, M. M. Odashima, and K. Capelle, Phys. Rev. B **81**, 125136 (2010).

[14] R. Peverati and D. G. Truhlar, J. Chem. Phys. **136**, 134704 (2012).

[15] V. N. Staroverov, G. E. Scuseria, J. Tao, and J. P. Perdew, Phys. Rev. B **69**, 075102 (2004).

[16] P. R. Antoniewicz and L. Kleinman, Phys. Rev. B **31**, 6779 (1985).

[17] J. P. Perdew, K. Burke, and M. Ernzerhof, Phys. Rev. Lett. **77**, 3865 (1996).

[18] J. P. Perdew, L. A. Constantin, E. Sagvolden, and K. Burke, Phys. Rev. Lett. **97**, 223002 (2006).

[19] A. Ruzsinszky, G. I. Csonka, and G. E. Scuseria, J. Chem. Theory Comput. **5**, 763 (2009).

[20] E. H. Lieb and S. Oxford, Int. J. Quantum Chem. **19**, 427 (1981).

[21] M. Levy and J. P. Perdew, Phys. Rev. B **48**, 11638 (1993).

[22] E. Fabiano, L. A. Constantin, and F. Della Sala, Phys. Rev. B **82**, 113104 (2010).

[23] É. Brémond, J. Chem. Phys. **145**, 244102 (2016).

[24] P. Haas, F. Tran, P. Blaha, and K. Schwarz, Phys. Rev. B **83**, 205117 (2011).

[25] E. Fabiano, L. A. Constantin, and F. Della Sala, J. Chem. Phys. **134**, 194112 (2011).

[26] E. Fabiano, L. A. Constantin, and F. Della Sala, Int. J. Quantum Chem. **113**, 673 (2013).

[27] D. C. Langreth and M. J. Mehl, Phys. Rev. Lett. **47**, 446 (1981).

[28] M. Levy and J. P. Perdew, Phys. Rev. A **32**, 2010 (1985).

[29] M. Levy, Phys. Rev. A **43**, 4637 (1991).

[30] D. J. Tozer, N. C. Handy, and W. H. Green, Chem. Phys. Lett. **273**, 183 (1997).

[31] D. J. Tozer and N. C. Handy, J. Chem. Phys. **108**, 2545 (1998).

[32] D. J. Tozer and N. C. Handy, J. Phys. Chem. A **102**, 3162 (1998).

[33] C. Adamo, M. Cossi, and V. Barone, J. Mol. Struct (Theochem.) **493**, 145 (1999).

[34] O. V. Gritsenko, P. R. T. Schipper, and E. J. Baerends, J. Chem. Phys. **107**, 5007 (1997).

[35] R. Peverati and D. G. Truhlar, J. Chem. Theory Comput. **8**, 2310 (2012).

[36] R. Peverati and D. G. Truhlar, Phys. Chem. Chem. Phys. **14**, 13171 (2012).

[37] W. Zhang, D. G. Truhlar, and M. Tang, J. Chem. Theory Comput. **9**, 3965 (2013).

[38] R. Peverati and D. G. Truhlar, Phil. Trans. R. Soc. A **372**, 20120476 (2014).

[39] H. S. Yu, W. Zhang, P. Verma, X. Heac, and D. G. Truhlar, Phys. Chem. Chem. Phys. **17**, 12146 (2015).

[40] E. Fabiano, L. A. Constantin, P. Cortona and F. Della Sala, J. Chem. Theory Comput. **11**, 122 (2015).

[41] S. Jana, A. Patra, L. A. Constantin, H. Myneni, and P. Samal, Phys. Rev. A **99**, 042515 (2019).

[42] S. Jana, A. Patra, L. A. Constantin, and P. Samal, J. Chem. Phys. **152**, 044111 (2020).

[43] S.-K. Ma and K. A. Brueckner, Phys. Rev. **165**, 18 (1968).

[44] M. Rasolt and D. J. W. Geldart, Phys. Rev. B **34**, 1325 (1986).

[45] C. D. Hu and D. C. Langreth, Phys. Rev. B **33**, 943 (1986).

[46] V. N. Staroverov, G. E. Scuseria, J. P. Perdew, E. R. Davidson, and J. Katriel, Phys. Rev. A **74**, 044501 (2006).

[47] J. P. Perdew, Phys. Rev. B **33**, 8822 (1986).

[48] J. P. Perdew, A. Ruzsinszky, G. I. Csonka, L. A. Constantin, and J. Sun, Phys. Rev. Lett. **103**, 026403 (2009).

[49] A. Cancio, G. P. Chen, B. T. Krull, and K. Burke, J. Chem. Phys. **149**, 084116 (2018).

[50] L. J. Sham, in *Computational Methods in Band Theory*, edited by P. M. Marcus, J. F. Janak, and A. R. Williams (Plenum Press, New York, 1971), p. 458.

[51] J. C. Pacheco-Kato, J. M. del Campo, J. L. Gázquez, S. B. Trickey, and A. Vela, Chem. Phys. Lett. **651**, 268 (2016).

[52] J. Carmona-Espíndola, J. L. Gázquez, A. Vela, and S. B. Trickey, J. Chem. Phys. **142**, 054105 (2015).

[53] E. Engel, J. A. Chevary, L. D. Macdonald, and S. H. Vosko, Z. Phys. D: At. Mol. Clusters **23**, 7 (1992).

[54] J. Carmona-Espíndola, J. L. Gázquez, A. Vela, and S. B. Trickey, J. Chem. Theory Comput. **15**, 303 (2019).

[55] See Supplemental Material at http://link.aps.org/supplemental/10.1103/PhysRevB.102.035129 for complete results calculated with the different functionals considered in this work.

[56] M. Valiev, E. J. Bylaska, N. Govind, K. Kowalski, T. P. Straatsma, H. J. J. van Dam, D. Wang, J. Nieplocha, E. Apra, T. L. Windus, and W. A. de Jong, Comput. Phys. Commun. **181**, 1477 (2010).

[57] J. M. del Campo, J. L. Gázquez, S. B. Trickey, and A. Vela, J. Chem. Phys. **136**, 104108 (2012).

[58] G. Kresse and J. Hafner, Phys. Rev. B **47**, 558 (1993); **49**, 14251 (1994).

[59] G. Kresse and J. Furthmüller, Comput. Mater. Sci. **6**, 15 (1996).

[60] G. Kresse and J. Furthmüller, Phys. Rev. B **54**, 11169 (1996).

[61] L. A. Constantin, E. Fabiano, S. Laricchia, and F. Della Sala, Phys. Rev. Lett. **106**, 186406 (2011).

[62] F. Tran, J. Stelzl, and P. Blaha, J. Chem. Phys. **144**, 204120 (2016).

[63] P. Haas, F. Tran, P. Blaha, K. Schwarz, and R. Laskowski, Phys. Rev. B **80**, 195109 (2009).

[64] F. Tran, R. Laskowski, P. Blaha, and K. Schwarz, Phys. Rev. B **75**, 115131 (2007).

[65] M. Ropo, K. Kokko, and L. Vitos, Phys. Rev. B **77**, 195445 (2008).

[66] P. Haas, F. Tran, and P. Blaha, Phys. Rev. B **79**, 085104 (2009); **79**, 209902(E) (2009).

[67] A. Savin, and E. R. Johnson, in *Judging Density-Functional Approximations: Some Pitfalls of Statistics*, edited by E. R. Johnson (Springer, New York, 2014), p. 81.

[68] J. P. Perdew and M. Levy, Phys. Rev. Lett. **51**, 1884 (1983).

[69] L. J. Sham and M. Schlüter, Phys. Rev. Lett. **51**, 1888 (1983).